

He II $\lambda 4686$ EMISSION IN THE SPECTRUM OF HDE 226868 (CYGNUS X-1)

G. A. H. WALKER AND S. YANG

Department of Geophysics and Astronomy, University of British Columbia

AND

J. W. GLASPEY

Département de Physique, Université de Montréal

Received 1978 March 20; accepted 1978 June 21

ABSTRACT

Thirteen image isocon spectra of HDE 226868 (Cyg X-1) have been analyzed, seven from a 4 month period in 1972 and six from a single cycle in 1975 September. The spectral type of HDE 226868 (O9.7 Ib [Walborn]) is intermediate between those of the two standards observed, HD 204172 (B0 Ib) and HD 209975 (O9.5 Ib). To compensate for the underlying absorption lines, we have subtracted mean spectra of (a) HD 204172 and (b) HD 209975, as observed in 1975, from the spectra of HDE 226868 after appropriately shifting the standard spectra to the absorption velocity curve of HDE 226868 (Bolton). The lines of O II are much stronger in the spectrum of HD 204172 than they are in either HDE 226868 or HD 209975, and they were reduced by a factor of 0.3 before subtraction. The resulting He II $\lambda 4686$ emission-line profiles indicate in both case *a* and case *b* that the emission in 1975 was only some 65% of its strength in 1972. The equivalent width shows a $\pm 20\%$ phase modulation, with a definite maximum near phase 0.65 and an apparent maximum near phase 0.1 in 1975 but not in 1972. He II emission velocity curves for cases *a* and *b* from 1972 and 1975 are consistent in showing a small ($\pm 30 \text{ km s}^{-1}$) systematically negative variation between phases 0.3 and 1.0 and values of -85 km s^{-1} and -75 km s^{-1} , respectively, at phase 0.1. Given the uncertainties of the technique, these results can only be considered indicative, but they strongly suggest that the He II $\lambda 4686$ emission is not directly associated with the region of the unseen secondary. Some of the velocity and equivalent width variations could be explained by a suitable phase dependence of the strength of the He II absorption in the spectrum of the primary.

Subject headings: stars: emission-line — stars: individual — X-rays: binaries

I. INTRODUCTION

A number of early-type spectroscopic binaries have been identified with X-ray sources. In each case the secondary appears to be a compact object such as a white dwarf or neutron star, with X-rays that are generated by accretion onto the secondary. In the case of Cygnus X-1 (HDE 226868) the secondary may be a black hole (see, for example, Eardley and Press 1975). The optical spectra of the primaries generally seem to be normal, apart from the presence of He II $\lambda 4686$ in emission and unusual H α emission. The excitation mechanism for He II $\lambda 4686$ emission is probably associated with the X-rays but is not clearly understood, even in the spectra of the Of stars where it is normally seen.

Early observations suggested that the He II $\lambda 4686$ emission in HDE 226868 might be the only optical feature unambiguously associated with the region of the secondary (although this was questioned by Smith, Margon, and Conti 1973) and consequently that it would provide a useful test for theoretical interpretations of the system. Most theories suggest that the

emission should come from close to the primary surface.

Photographic spectroscopic observations (Walborn 1973; Bolton 1972) suggested that the He II $\lambda 4686$ emission was visible only at the extreme photometric phases of 0.1 and 0.6, but Hutchings *et al.* (1973) demonstrated from image isocon spectra taken in 1972 that, when account was taken of the expected He II $\lambda 4686$ absorption line in the spectrum of the primary, emission was visible at all phases and was less variable in strength than supposed. Further, the line showed a greater velocity amplitude than did the absorption velocity curve of the primary and was some 120° out of phase with it.

In 1975 we obtained another series of image isocon spectra of HDE 226868 and the standard stars HD 204172 and HD 209975 (19 Cephei) on six consecutive nights. These data are of similar or better quality than those obtained in 1972 and have the advantage of covering a single cycle of the 5.6 day period, which avoids possible confusion with cycle-to-cycle variations. In this paper we combine the best of the 1972 spectra and all those of 1975, and we reexamine the

TABLE 1
ISOCON OBSERVATIONS OF CYGNUS X-1 (HDE 226868)

UT Date	Exposure (minutes)	JD (2,440,000+)	Phase	Abs. Line Vel.* (km s ⁻¹)	Photometric Phase
1972:					
July 17.....	73	1515.763	0.723	-47.27	0.882
July 18.....	90	1516.763	0.906	+31.47	0.061
July 19.....	66	1517.763	0.095	+73.84	0.239
August 1.....	84	1530.896	0.438	-43.48	0.585
August 2.....	74	1531.838	0.598	-70.04	0.753
August 4.....	51	1533.890	0.968	+55.38	0.119
October 8.....	74	1598.646	0.532	-66.09	0.683
1975:					
September 10.....	54	2665.720	0.094	+73.90	0.238
September 11.....	120	2666.732	0.278	+22.41	0.419
September 12.....	72	2667.795	0.461	-50.63	0.609
September 13.....	128	2668.768	0.626	-68.32	0.783
September 14.....	140	2669.708	0.791	-20.81	0.951
September 15.....	86	2670.698	0.976	+57.98	0.127

* Bolton 1975.

question of the He II and other absorption-line compensation.

II. OBSERVATIONS AND REDUCTIONS

All of the observations in the region of He II $\lambda 4686$ which are used in this discussion are listed in Table 1. Three of the spectra taken in 1972 and discussed by Hutchings *et al.* (1973) (July 14, July 15, and October 7) are not included, as they are of inferior quality. Phase and absorption-line velocity were computed from the ephemeris by Bolton (1975).

Each of the spectra was obtained with a refrigerated English electric P850 image isocon television camera at 2.4 \AA mm^{-1} in the coude spectrograph of the DAO 1.2 m telescope. Details of the technique are given in Buchholz *et al.* (1973). An analog charge pattern corresponding to the spectrum was allowed to build up in the camera target, and this was read out and digitized after a suitable integration time. The sensitivity and linearity of the tube were improved by a low-light-level

flash at the start of each integration. Some 30–40 individual exposures are included in each spectrum listed in Table 1.

Each spectrum has been filtered to 20% of the Nyquist frequency corresponding roughly to a five-point running mean, which is equivalent to a resolution of 0.3 mm or 0.7 \AA in the spectrum.

A wavelength calibration was provided on each night by spectra of HD 204172. Shifts of between one and three points have been applied to the spectra of 1975 September 11, 12, and 14 to compensate for short-term scanning raster displacements determined from the fiducial marks.

One of the untreated filtered spectra is shown in Figure 1. The curvature is due in part to the isocon response and in part to the spectral energy distribution in HDE 226868. The fiducial marks at either end of the spectrum were formed by masking the photocathode.

The spectral region covered contains a large number

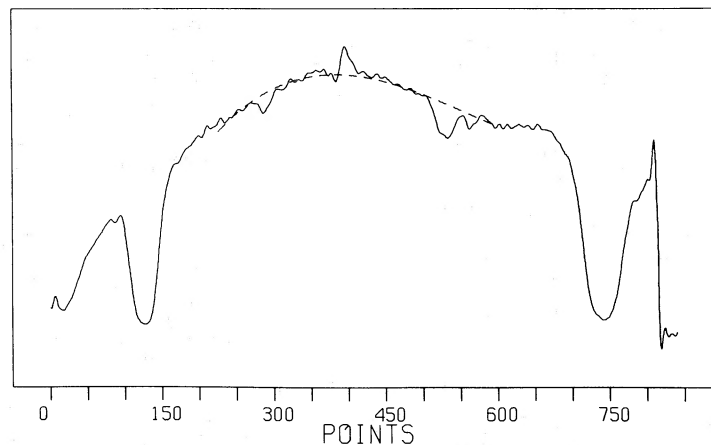


FIG. 1.—An example of an isocon spectrum of HDE 226868 (Cyg X-1) covering the spectral region $\lambda\lambda 4635\text{--}4720$ after filtering to 20% of the Nyquist frequency and removal of dark current. Fiducial marks formed by masking the photocathode are seen at either end. Spectral curvature is caused by instrumental response and interstellar reddening and was removed to a first order by fitting a third-order polynomial as shown by the dashed line.

of weak absorption features, particularly those due to O II, and it is not clear that the stellar continuum can be defined at more than a few points. Between five and seven points were chosen between the fiducial marks at similar wavelengths in each spectrum, and a third-order polynomial was fitted through the points except for the spectrum of 1972 July 17, which shows an apparently broad enhancement on the short-wavelength side of $\lambda 4686$; this could be emission but was treated to some extent as continuum by the use of a fourth-order polynomial. It was felt in the other cases that, by restricting the fit to a third-order polynomial, instrumental and interstellar spectral curvature would be removed to a first order while subjective fitting and possible oscillations in higher-order curves, which might eliminate some of the lower-frequency information in the data, would be minimized. (One such fit is shown in Fig. 1.)

All 13 spectra of HDE 226868, calibrated in wavelength and normalized to their respective continua, are plotted in order of phase in Figure 2. Mean normalized spectra from the 1975 observations of the standard stars HD 204172 and HD 209975 are plotted in Figure 3. The principal spectral features are indicated.

The absorption-line velocity variations in the primary of HDE 226868 can be seen in the $\lambda 4640$ blend of N II, Si IV, and O II and in the line of He I $\lambda 4713.1$. The nature of some of the variations in the He II $\lambda 4686$ emission can be seen. In 1972 emission can be seen at all phases except conjunction. It is particularly prominent at the absorption-line velocity extrema in both

1972 and 1975, with absorption in either the red or violet wings. These effects are also evident in the photographic spectra published by Walborn (1973).

III. ANALYSIS

Walborn (1973) has shown convincingly that the spectrum of HDE 226868 with the notable exception of He II $\lambda 4686$ is that of an O9.7 Iab star, intermediate between 19 Cephei (O9.5 Ib) and ϵ Orionis (B0 Ia). One would expect, therefore, that the He II $\lambda 4686$ absorption line in the primary of HDE 226868 might be stronger than that in HD 204172 (B0 Ib) and more similar to that in 19 Cephei (HD 209975). From Figure 3 one finds that the He II $\lambda 4686$ absorption is in fact about 30% stronger in 19 Cephei than in HD 204172 (13.3% and 10.5% central depths, respectively).

The absorption lines of O II on the other hand are much weaker in the spectrum of HD 200995, as they have only some 30% of the strength they display in the spectrum of HD 204172, and in fact closely resemble their strength in the spectrum of HDE 226868. These lines vary quite widely between individual stars, as they are sensitive, for example, to luminosity.

The spectrum of HD 204172 varies significantly, particularly over the 4 month period covered by the 1972 observations. Consequently, in order to form a standard spectrum with which to compare those of HDE 226868, we have taken a mean of the 1975 HD 204172 spectra only, and the individual O II absorption-line strengths have been reduced to 0.3 of their value. A

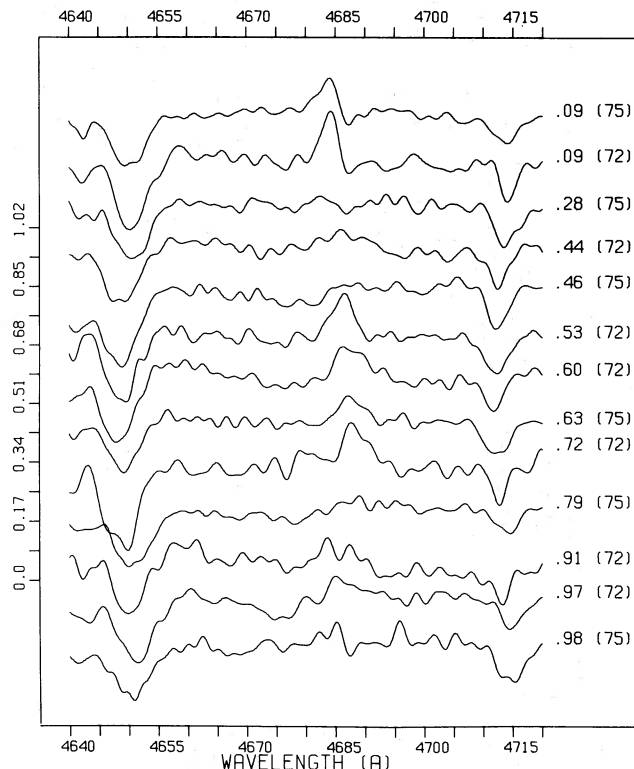


FIG. 2.—The 13 spectra of HDE 226868 (Cyg X-1), rectified to continua and calibrated in wavelength

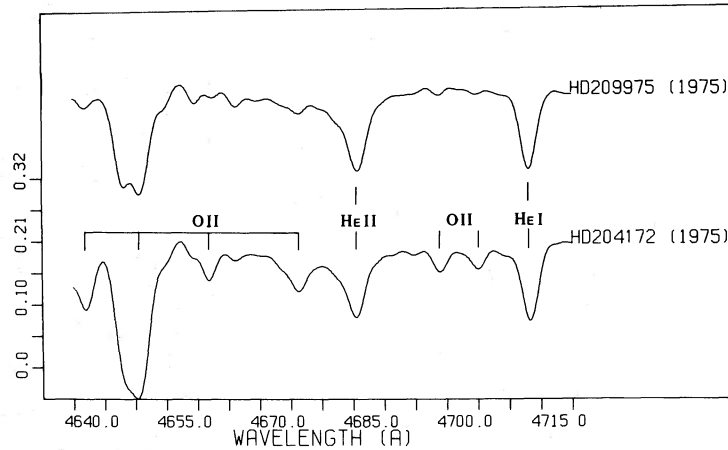


FIG. 3.—Mean, normalized spectra of the standards HD 204172 (B0 Ib) and HD 209975 (O9.5 Ib), with the principal absorption lines identified.

mean of the spectra of HD 209975 from 1975 has also been formed without changing the strengths of the individual absorption lines.

Difference spectra in the sense (HDE 226868) minus (standard) have been formed after shifting the standard spectrum to conform to Bolton's (1975) absorption-line

velocity curve of the primary. The difference spectra are plotted in Figures 4 and 5 using (case *a*) HD 204172 (O II absorption lines reduced by 0.3) and (case *b*) HD 209975 (unaltered) as standard over the wavelength interval $\lambda\lambda 4655\text{--}4720$. An enlargement of the profiles for the region $\lambda\lambda 4570\text{--}4700$ is shown in Figures 6 and

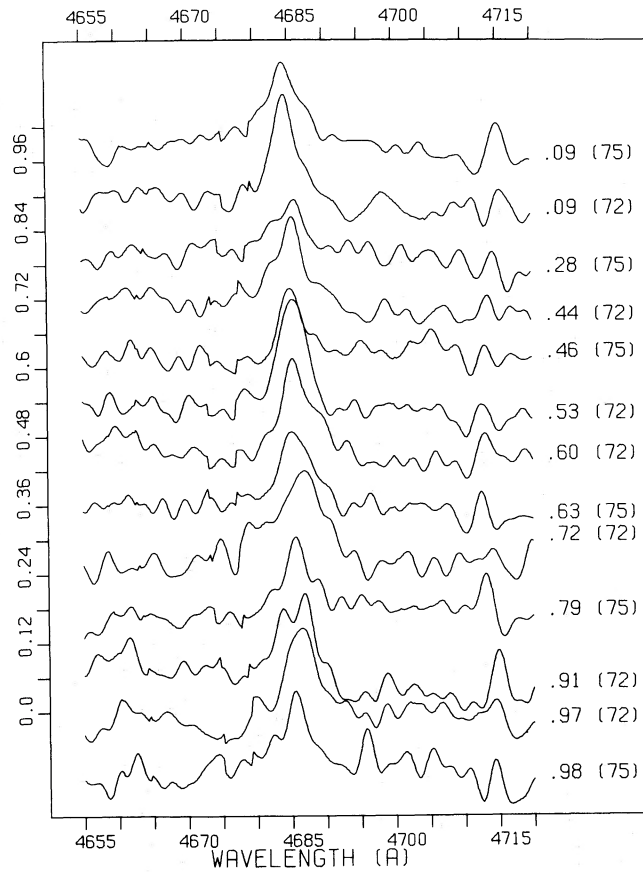


FIG. 4.—Difference spectra in the sense (case *a*) (HDE 226868) minus (HD 204172) after shifting the spectrum of HD 204172 to the appropriate absorption-line velocity (Bolton 1975) and reducing the strength of the O II absorption lines in HD 204172 to 30% of their original value.

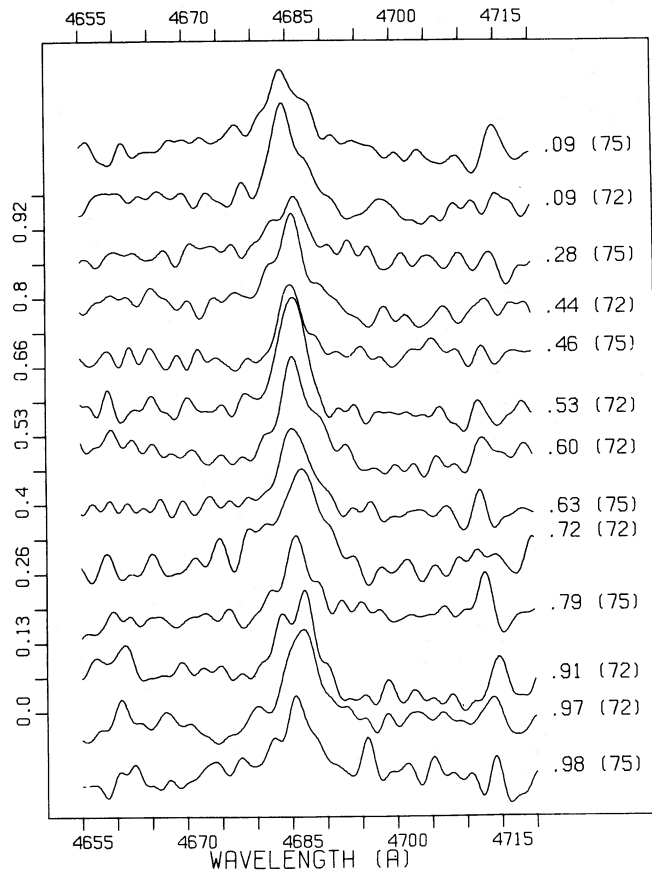


FIG. 5.—Difference spectra in the sense (case *b*) (HDE 226868) minus (HD 209975) after shifting the spectrum of HD 209975 to the appropriate absorption-line velocity (Bolton 1975). Note the difference in vertical scale compared to Fig. 4.

7. The short vertical marks indicate the wavelength of the centroid of the He II $\lambda 4686$ emission-line profile. The continuous vertical line indicates $\lambda 4685.6$, the He II rest wavelength. The horizontal dashed lines indicate the adopted continua used in estimating the emission-line equivalent widths and centroids.

Wavelength integration limits for equivalent width and centroid measurements were established by estimating triangles of best fit to the observed emission-line profiles. These limits were approximately $\pm 7 \text{ \AA}$ from the peak of each line. The equivalent widths and corresponding velocities of the emission-line centroids are listed in Table 2.

IV. He II $\lambda 4686$ EMISSION-LINE EQUIVALENT WIDTHS

The equivalent widths in angstroms are plotted in Figures 8 and 9 (cases *a* and *b*, respectively) as a function of phase, with the observations of 1972 shown as asterisks and those of 1975 as circles. The variations are very similar in Figures 8 and 9 and in 1975 and 1972, apart from differences in scale and the two points at phase 0.1. If we exclude the latter, the 1975 equivalent widths are only some 65% of those in 1972.

In Figure 10 the 1975 equivalent widths of Figure 8 have been amplified by a factor 1.7. A well-defined maximum seen near phase 0.6 is evident in the separate

1975 and 1972 data, and can probably be considered significant. The behavior of the points at phase 0.1—one from 1972, the other from 1975—is ambiguous. These two line profiles are among the best defined and also show closely similar radial velocities. Either the equivalent width at this phase is immune to cycle-to-cycle variations, or the strength is anomalous for one of the points. This can be clarified only by further observations.

V. RADIAL VELOCITY VARIATIONS OF THE He II $\lambda 4686$ EMISSION

The radial velocity variations for cases *a* and *b* are plotted as a function of phase in Figures 11 and 12, respectively. The 1972 results are shown by asterisks, and those for 1975 by circles. While the 1972 and 1975 results appear well correlated in both figures, the 1975 velocities show a smaller range and apparently smoother variation with phase.

Figures 11 and 12 both show a significant negative velocity of between -70 and -95 km s^{-1} at phase 0.1 which is not matched by a correspondingly large positive velocity, although the curves do reach a shallow maximum of about $+10 \text{ km s}^{-1}$ near phase 0.6–0.7.

While the scatter in the points probably reflects the

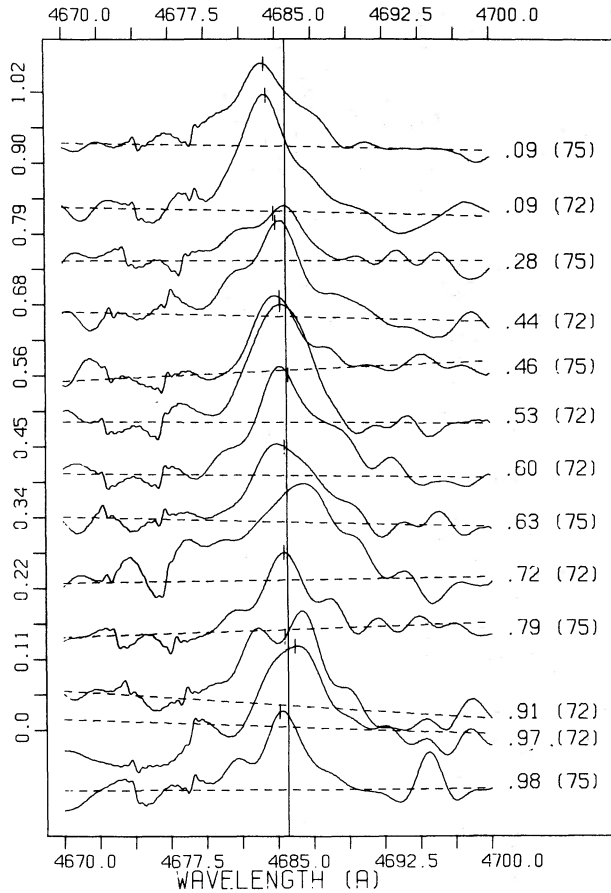


FIG. 6.—Enlargement of the He II $\lambda 4686$ emission profiles in HDE 226868 (Cyg X-1) from Fig. 4. The short vertical marks indicate the centroid of the emission-line profile. The continuous vertical line at $\lambda 4685.6$ is the rest wavelength of the He II line, and the dashed horizontal line is the continuum level adopted.

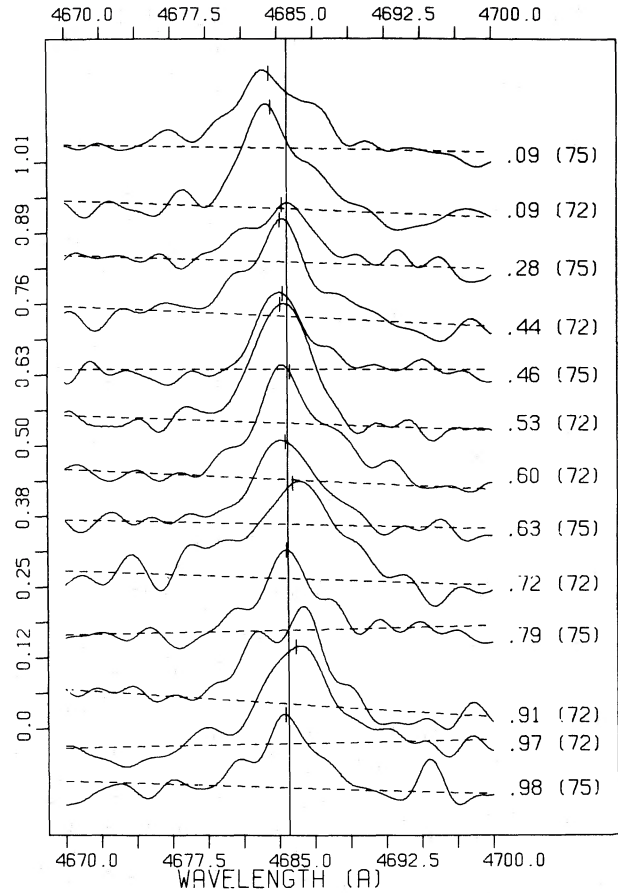


FIG. 7.—Enlargement of the He II $\lambda 4686$ emission profiles in HDE 226868 (Cyg X-1) from Fig. 5. The short vertical marks indicate the centroid of the He II emission-line profile. The continuous vertical line at $\lambda 4685.6$ is the rest wavelength of the He II line, and the dashed horizontal line is the adopted continuum level.

TABLE 2
CYGNUS X-1 He II $\lambda 4686$ EQUIVALENT WIDTHS AND VELOCITIES

PHASE	EW (Å)		RADIAL VELOCITY \ddagger (km s $^{-1}$)		DATE
	a^*	b^\dagger	a^*	b^\dagger	
0.094.....	0.72	0.88	-94.0	-79.5	1975 Sept 10
0.095.....	0.85	0.94	-84.0	-73.2	1972 July 19
0.278.....	0.42	0.57	-53.7	-22.2	1975 Sept 11
0.438.....	0.75	0.94	-42.7	-33.0	1972 Aug 1
0.461.....	0.48	0.58	-28.2	-19.7	1975 Sept 12
0.532.....	0.92	1.08	-25.5	-32.0	1972 Oct 8
0.598.....	0.97	1.20	+8.5	+10.5	1972 Aug 2
0.626.....	0.66	0.85	-9.5	-9.2	1975 Sept 13
0.723.....	1.26	1.31	+1.0	+22.7	1972 July 17
0.791.....	0.53	0.64	-15.0	-7.2	1975 Sept 14
0.906.....	0.86	0.96	-13.5	-0.5	1972 July 18
0.968.....	0.58	1.07	+32.5	+34.5	1972 Aug 4
0.976.....	0.54	0.60	-36.0	-13.2	1975 Sept 15

* Case a based on profiles from difference spectra in the sense (HDE 226868) minus (HD 204172), with absorption lines of O II reduced to 30% in HD 204172.

\dagger Case b based on difference spectra in the sense (HDE 226868) minus (HD 209975).

\ddagger Estimated from the center of gravity of the emission-line profile.

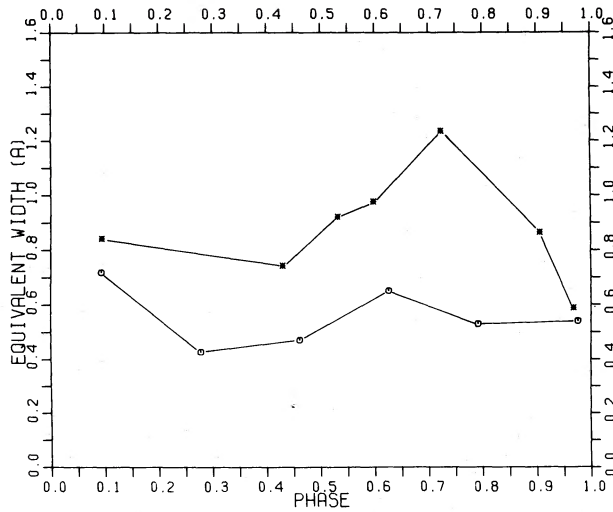


FIG. 8.—The equivalent widths in angstroms of the emission profiles of He II $\lambda 4686$ from Fig. 6, plotted against absorption-line phase for HDE 226868 (Cyg X-1) for case *a*. Data from 1972 are shown as asterisks and from 1975 as circles.

internal precision of the velocities, the assumptions in the difference spectrum technique imply potentially large errors. The He II $\lambda 4686$ absorption-line profile is not symmetric in the spectra of either HD 204172 or HD 209975, which would introduce a systematic error in location of the center of gravity of the emission-line profile. While compensation for the O II absorption lines in the spectrum of HDE 226868 is fairly complete, which allows a continuum to be established outside the region of the emission line in the difference spectrum, the estimation of two separate sets of continua, particularly the first one in the raw data, and finally in

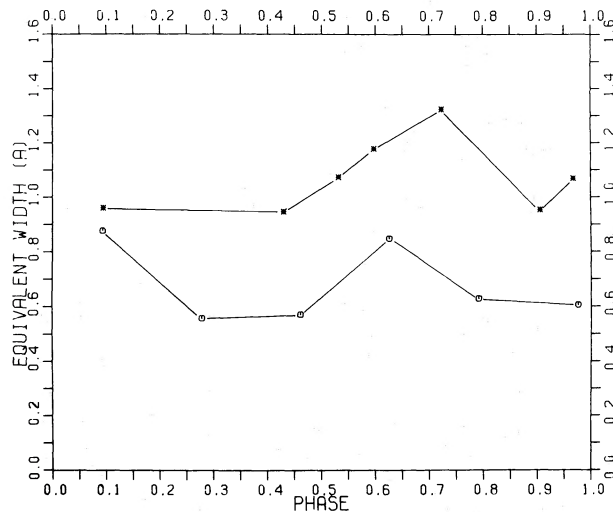


FIG. 9.—The equivalent widths in angstroms of the emission profiles of He II $\lambda 4686$ from Fig. 7, plotted against absorption-line phase for HDE 226868 (Cyg X-1) for case *b*. Data from 1972 are shown as asterisks and from 1975 as circles.

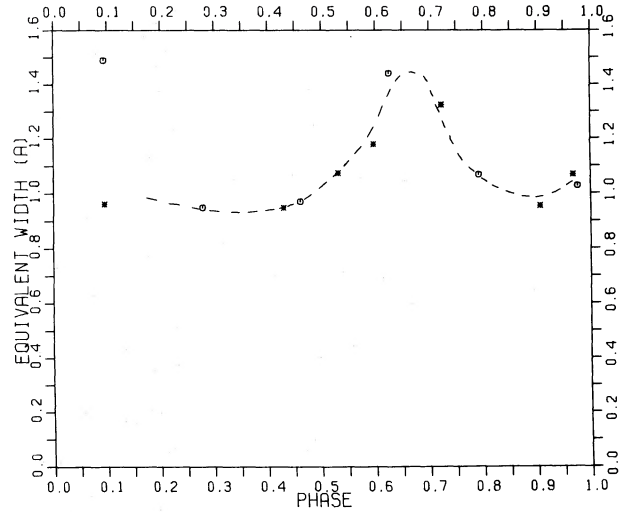


FIG. 10.—The same as Fig. 9, except that the 1975 equivalent widths have been amplified by a factor of 1.7.

the difference spectrum, must introduce further systematic effects.

There is some evidence from the He I $\lambda 4713$ line that the lines in HDE 226868 are broader and shallower than in either standard, which, if this also applies to the He II $\lambda 4686$ absorption in the primary, will also lead to a distortion of the emission-line profile.

If one increases the strength of the He II $\lambda 4686$ absorption profile which is subtracted from the spectra of HDE 226868, the velocity excursions in Figure 11 or 12 are reduced. In particular, if the central depth is increased by a factor of 1.1, the velocity at phase 0.1 is reduced by approximately 10 km s^{-1} . Consequently, if the He II $\lambda 4686$ absorption-line strength for the

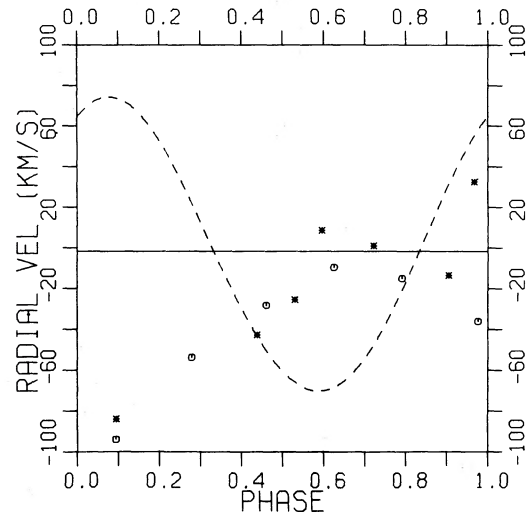


FIG. 11.—Radial velocities determined from the centers of gravity of the He II $\lambda 4686$ emission profiles of Fig. 6, plotted against phase for case *a*. Asterisks are for the 1972 data and circles for 1975. The dashed curve is the absorption-line velocity curve of the primary, adopted from Bolton (1975).

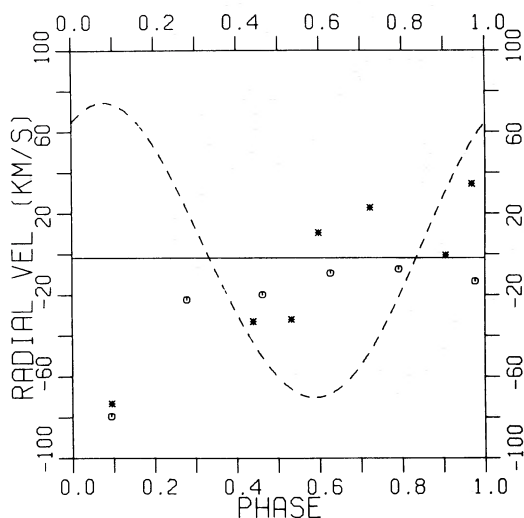


FIG. 12.—Radial velocities determined from the centers of gravity of the He II $\lambda 4686$ emission profiles of Fig. 7, plotted against phase for case *b*. Asterisks are for the 1972 data and circles for 1975. The dashed curve is the absorption-line velocity curve of the primary, adopted from Bolton (1975).

primary is suitably phase dependent, this, in conjunction with a stationary emission line, could also give rise to velocity curves such as those in Figures 10 and 11. It is interesting that Smith, Margon, and Conti (1973) did find that the spectral type of HDE 226868 varied with phase between O9.5 and B0 and, in particular, that the He II $\lambda 4541$ absorption line varied in strength. The qualitative variations with phase they have tabulated correspond roughly to the behavior which could be responsible for the results shown in Figures 10 and 11.

VI. He I $\lambda 4713$ LINE

In the difference spectra shown in Figures 4 and 5, a peak accompanied by shallow wings is seen at the wavelength of the He I $\lambda 4713$ line in the spectrum of the primary for most cases, except perhaps that for phase 0.791 (where a velocity shift is indicated). This implies that the absorption line is shallower and broader but of approximately the same equivalent width as that in the standards. There is no obvious systematic asymmetry evident with phase.

Bolton, C. T. 1972, *Nature*, **235**, 271.
 ———. 1975, *Ap. J.*, **200**, 269.

Buchholz, V., Walker, G. A. H., Auman, J. R., and Isherwood, B. I. 1973, *Astronomical Observations with Television-Type Sensors*, ed. J. Glaspey and G. A. H. Walker (Vancouver: University of British Columbia), p. 199.
 Eardley, D. M., and Press, W. H. 1975, *Ann. Rev. Astr. Ap.*, **13**, 381.

JOHN W. GLASPEY: Département de Physique, Université de Montréal, P.O. Box 6128, Montréal, P.Q., H3C 3J7, Canada

GORDON A. H. WALKER and STEPHENSON YANG: Department of Geophysics and Astronomy, University of British Columbia, Vancouver, B.C., V6T 1W5, Canada

VII. CONCLUSIONS

These results do not seem to support the large velocity changes of the He II $\lambda 4585$ emission line determined by Hutchings *et al.* (1973) from the 1972 data. In that paper HD 204172 alone was used as a standard, both with all absorption lines reduced by 20% and unaltered. For this analysis we rejected three of the 1972 sets of observations as being of too poor quality. Further, the O II $\lambda 4676.2$ absorption line modifies the blue wing of the He II $\lambda 4685.6$ emission line quite strongly and has been reduced to only 30% of its value in HD 204172 for this analysis. In addition, the absorption-line intensities in the spectra of HD 204172 were quite variable in 1972, and we have preferred a mean spectrum based on the 1975 observations, which seems to be supported by the HD 209975 comparison. The spectral type given by Walborn (1973) also supports the larger strength of the He II underlying absorption adopted in this paper.

The radial velocities in this paper were measured from the center of gravity of each profile. If the maxima of the profiles are used instead, it can be seen from Figures 9 and 10 that the scatter in the velocities is increased without significantly changing the behavior seen in Figures 11 and 12. The only profile to show a large discrepancy is that for phase 0.723, for which some difficulty was experienced in fitting a continuum. The velocity of the peak is approximately $+70 \text{ km s}^{-1}$. However, this single large value is not supported by the peak velocities at the two nearby phases of 0.629 and 0.791. In view of the character of the noise after filtering to 20% of the Nyquist frequency, the peak velocities must be considered less trustworthy.

In view of the uncertainties introduced by the assumptions in the analysis and discussed above, we do not propose a model to account for the behavior of the He II $\lambda 4686$ emission shown in Figures 8, 9, 10, 11, and 12. Nonetheless, it appears very likely that, as Smith, Margon, and Conti (1973) have already suggested, the emission does not arise in the region of the secondary.

This work was supported by research funds from the Canadian NRC. It is a pleasure to thank Dr. G. G. Fahlman for the use of a number of his programs, Dr. J. R. Auman for many helpful discussions, and Dr. C. T. Bolton for useful comments on the paper in manuscript.

REFERENCES

Hutchings, J. B., Crampton, D., Glaspey, J., and Walker, G. A. H. 1973, *Ap. J.*, **182**, 549.
 Smith, H. E., Margon, B., and Conti, P. S. 1973, *Ap. J. (Letters)*, **179**, L125.
 Walborn, N. R. 1973, *Ap. J. (Letters)*, **179**, L123.